Adipose tissue-specific inactivation of the retinoblastoma protein protects against diabesity because of increased energy expenditure

Nassim Dali-Youcef*†, Chikage Mataki*, Agnès Coste*, Nadia Messaddeq*, Sylvain Giroud‡, Stéphane Blanc‡, Christian Koehl†, Marie-France Champy§, Pierre Chambon*, Lluis Fajas¶, Daniel Metzger*, Kristina Schoonjans*, and Johan Auwerx*†§‖

*Institut de Génétique et de Biologie Moléculaire et Cellulaire de Strasbourg, Institut National de la Santé et de la Recherche Médicale, Centre National de la Recherche Scientifique, Université Louis Pasteur, 1 Rue Laurent Fries, BP 10142, 67404 Illkirch, France; †Laboratoire de Biochimie Générale et Spécialisée, Hôpitaux Universitaires de Strasbourg, 1 Place de l'Hôpital, 67098 Strasbourg Cedex, France; ‡Département d'Ecologie, Physiologie et Ethologie, Institut Pluridisciplinaire Hubert Curien, Centre National de la Recherche Scientifique Unité Mixte de Recherche 7178 and Université Louis Pasteur, 23 Rue Becquerel, 67087 Strasbourg Cedex 02, France; §Institut Clinique de la Souris, Genopole Strasbourg, 67404 Illkirch, France; and ¶Metabolism and Cancer Laboratory, Le Centre Régional de Lutte Contre le Cancer Val d'Aurelle, Parc Euromédecine U540, 208 Rue des Apothicaires, F-34298 Montpellier Cedex 05, France

Edited by Bruce M. Spiegelman, Harvard Medical School, Boston, MA, and approved May 3, 2007 (received for review December 26, 2006)

The role of the tumor suppressor retinoblastoma protein (pRb) has been firmly established in the control of cell cycle, apoptosis, and differentiation. Recently, it was demonstrated that lack of pRb promotes a switch from white to brown adipocyte differentiation *in vitro*. We used the Cre-Lox system to specifically inactivate pRb in adult adipose tissue. Under a high-fat diet, pRb-deficient ($pRb^{ad-/-}$) mice failed to gain weight because of increased energy expenditure. This protection against weight gain was caused by the activation of mitochondrial activity in white and brown fat as evidenced by histologic, electron microscopic, and gene expression studies. Moreover, $pRb^{-/-}$ mouse embryonic fibroblasts displayed higher proliferation and apoptosis rates than $pRb^{+/+}$ mouse embryonic fibroblasts, which could contribute to the altered white adipose tissue morphology. Taken together, our data support a direct role of pRb in adipocyte cell fate determination *in vivo* and suggest that pRb could serve as a potential therapeutic target to trigger mitochondrial activation in white adipose tissue and brown adipose tissue, favoring an increase in energy expenditure and subsequent weight loss.

brown adipose tissue | mitochondria | pocket proteins | obesity

The retinoblastoma protein (pRb), product of the first tumor suppressor gene to be characterized, belongs to the family of pocket proteins composed of pRb, p107, and p130 proteins. Pocket proteins play an important role in cell cycle regulation because they induce growth arrest through their interaction with other transcription factors such as E2Fs (reviewed in refs. 1 and 2). The proteins are also involved in the control of apoptosis (3) and cell differentiation (2, 4). Although pocket proteins have redundant functions in cell cycle progression, pRb is thought to play the most important role in cell differentiation. Indeed, pRb germ-line knockout animals die prematurely because of developmental defects comprising lack of differentiation of brain, skeletal muscle, lens, and cells of the erythropoietic lineage (5–7). Furthermore, it has been demonstrated that pRb is also essential for late osteoblast differentiation and chondrocyte maturation (8) and for proper skin differentiation (9, 10).

Recently, a growing amount of evidence, mainly obtained from the characterization of cell culture models, has suggested a dual role of pRb in adipocyte differentiation. Indeed, it was suggested that pRb facilitates the differentiation of preadipocytes and mouse embryonic fibroblasts (MEFs) into adipocytes (11–13). Another study showed that $pRb^{-/-}$ 3T3 cells fail to undergo terminal differentiation when grown in the appropriate differentiating medium and that overexpression of pRb promotes adipocyte differentiation in wild-type cells (14). Moreover, the simian virus 40 large antigen blocks adipocyte differentiation of 3T3-L1 cells by inhibiting pRb's positive effect on differentiation (15). In addition to these studies, our group has recently suggested an inhibitory role of pRb at particular stages of adipocyte differentiation, through the recruitment of the histone deacetylase HDAC3 to the nuclear receptor peroxisome proliferator-activated receptor γ (16). Consistent with these findings, transgenic mice overexpressing pRb show a significant decrease in paraovarian fat pad mass (17). It seems, therefore, that pRb plays a dual role in adipocyte differentiation. During the clonal expansion and the early stages of adipocyte differentiation, pRb inhibits adipocyte differentiation (16). Thereafter, pRb rather activates adipogenesis by allowing the cells to exit the cell cycle for terminal differentiation (18).

In addition to its impact on adipocyte differentiation, pRb was also proposed to act as a molecular switch between white adipose tissue (WAT) and brown adipose tissue (BAT) differentiation. $pRb^{-/-}$ MEFs display characteristics of BAT, with activation of BAT-specific genes, such as the uncoupling protein 1 (UCP1) and the peroxisome proliferator-activated receptor γ coactivator 1α (PGC-1α), and an increase in mitochondria number (13). These observations are in line with older data from transgenic mice overexpressing the simian virus 40 antigen specifically in WAT, in which impaired pRb activity leads to the conversion of WAT into BAT (19). Furthermore, a recent study reported that in $p107^{-/-}$ mice, WAT is poorly differentiated with enhanced expression of UCP1 and PGC-1α. Interestingly, in these $p107^{-/-}$ preadipocytes, pRb levels were also robustly reduced (11).

Although a wealth of evidence suggests that pRb influences adipocyte differentiation *in vitro*, its role in the regulation of adipocyte cell fate determination has not been yet explored *in vivo*. In the present study, we used the loxP-$CreER^{T2}$ technology to demonstrate that specific ablation of pRb in adult adipose tissue leads to mitochondrial activation in WAT and BAT, which protects $pRb^{ad-/-}$ mice from diet-induced obesity.

Author contributions: N.D.-Y. and J.A. designed research; N.D.-Y., C.M., A.C., and N.M. performed research; S.G., S.B., M.-F.C., L.F., and K.S. contributed new reagents/analytic tools; N.D.-Y., C.K., P.C., D.M., and J.A. analyzed data; and N.D.-Y. and J.A. wrote the paper.

The authors declare no conflict of interest.

This article is a PNAS Direct Submission.

Abbreviations: MEF, mouse embryonic fibroblast; CFSE, 5- (and 6)-carboxyfluorescein diacetate succinimidyl ester; WAT, white adipose tissue; BAT, brown adipose tissue; HFD, high-fat diet; ORO, Oil red-O; PI, propidium iodide; PGC-1α and -β, peroxisome proliferator-activated receptor γ coactivator 1α and -β.

‖To whom correspondence should be addressed. E-mail: auwerx@igbmc.u-strasbg.fr.

This article contains supporting information online at www.pnas.org/cgi/content/full/0611568104/DC1.

PHYSIOLOGY

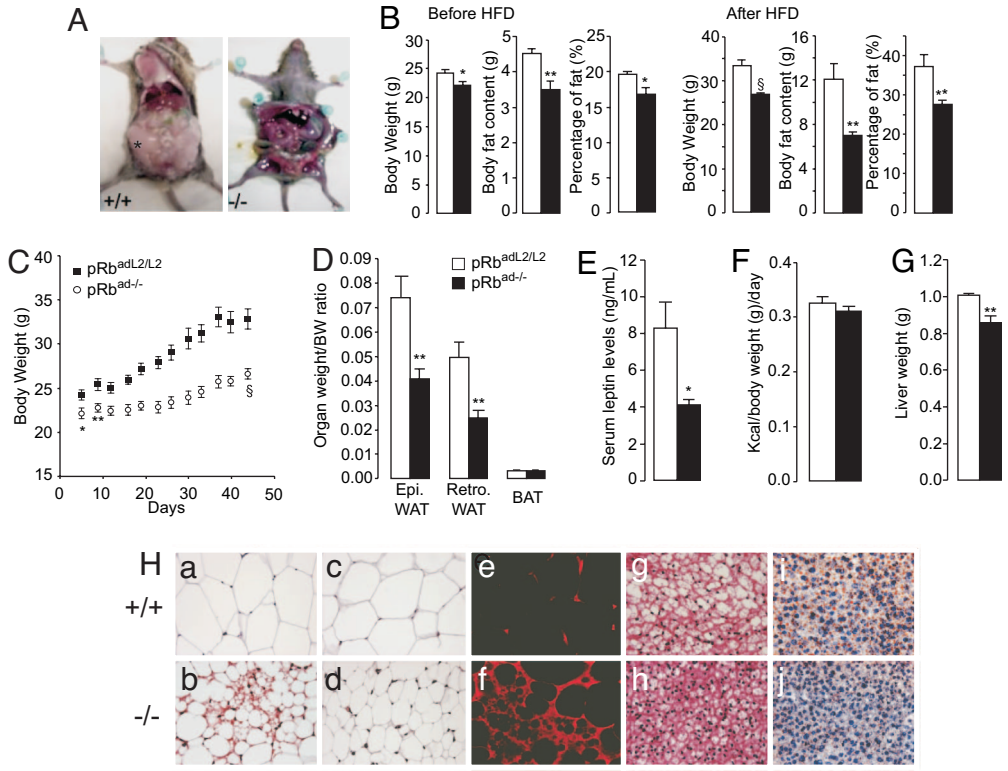

Fig. 1. pRb deletion prevents weight gain in mice fed a HFD. (*A*) HFD induces inguinal and retroperitoneal fat accumulation (*) in $pRb^{adL2/L2}$ mice as compared with $pRb^{ad-/-}$ animals, in which the white fat furthermore also exhibited a redish aspect. Upon HFD, livers from control mice were pale because of lipid accumulation, whereas pRb-deleted mice livers were dark red. (*B*) Body weight and dual energy x-ray absorptiometry of body fat content and the percentage of fat 5 days (before HFD) and 6 weeks (after HFD) after tamoxifen to induce adipose-specific pRb deletion ($n = 6$ animals per group). (*C*) Body weight progression in $pRb^{adL2/L2}$ (filled squares) and $pRb^{ad-/-}$ mice (open circles) during 45 days of HFD. (*D*) Comparison of epididymal (epi) WAT, retroperitoneal (retro) WAT, and BAT weights/body weights (BW) between $pRb^{ad-/-}$ and $pRb^{adL2/L2}$ mice. (*E*) Changes in serum leptin levels between $pRb^{ad-/-}$ and control mice after 45 days of HFD. (*F*) Food intake of pRb-deficient and control mice during 1 month of HFD. (*G*) Liver weights of $pRb^{ad-/-}$ and $pRb^{adL2/L2}$ mice under HFD. (*H*) H&E staining of epididymal WAT (*a* vs. *b*), retroperitoneal WAT (*c* vs. *d*), and BAT sections (*g* vs. *h*), immunohistochemistry of WAT sections using an anti-OPA-1 antibody, a mitochondrial protein (*e* vs. *f*), and ORO staining of liver sections (*i* vs. *j*) in $pRb^{ad-/-}$ versus control mice under HFD. *, $P < 0.05$; **, $P < 0.01$; §, $P < 0.001$.

Results

$pRb^{ad-/-}$ Animals Exhibit a Lean Phenotype After High-Fat Feeding. Because pRb was previously shown to be involved in body weight determination, we analyzed body weight evolution in animals in which we induced an adipocyte-specific ablation of pRb in adulthood. We therefore crossed mice in which the pRb allele was flanked by loxP sites (20) with mice that express the Cre-ER^{T2} recombinase in adipose tissue (21) and generated cohorts of bigenic $pRb^{L2/L2} \times aP_2$Cre-$ER^{T2(Tg/0)}$ on a C57BL6/J background. To induce deletion of the pRb gene in WAT, these mice ($n = 8$) were injected i.p. at the age of 6 weeks with tamoxifen at 50 mg/kg per day for 5 consecutive days [supporting information (SI) Fig. 6]. Mice in which pRb was inactivated after tamoxifen injection will be referred to as $pRb^{ad-/-}$, and their controls will be referred to as $pRb^{adL2/L2}$. After the last tamoxifen injection, a modest but significant decrease in the body weight of $pRb^{ad-/-}$ was observed as compared with $pRb^{adL2/L2}$ mice ($P = 0.028$) (Fig. 1*B*). The decrease in body weight was paralleled by a significant decrease in the body fat content ($P = 0.005$) and the percentage of fat ($P = 0.028$) as determined by dual energy x-ray absorptiometry (Fig. 1*B*). Mice were then fed a high-fat diet (HFD) for 6 weeks and morphometric analysis was repeated. Under HFD, the $pRb^{adL2/L2}$ mice gained weight, whereas the $pRb^{ad-/-}$ mice were protected from excessive weight gain (Fig. 1*C*). Dual energy x-ray absorptiometry performed 6 weeks after the initiation of the HFD indicated a significant difference in the body fat content in $pRb^{ad-/-}$ as compared with $pRb^{adL2/L2}$ animals (Fig. 1*B*). The weight of the different fat pads and serum leptin levels were also significantly lower in $pRb^{ad-/-}$ mice (Fig. 1 *A*, *D*, and *E*). Whereas fasting serum glucose and glucose tolerance tests were not significantly different between the two genotypes, serum insulin levels were decreased, although the difference just failed to reach statistical significance ($P = 0.053$; SI Fig. 7). Serum lipid and adiponectin levels were not different (SI Fig. 7). There was no change in food intake between pRb-deficient mice and their control littermates (Fig. 1*F*). The reduced liver weight reflected the decreased fat accumulation in the liver of $pRb^{ad-/-}$ animals (Fig. 1*G*).

BAT Transformation of WAT and Increased Energy Expenditure in $pRb^{ad-/-}$ Animals. H&E staining of WAT sections obtained from HFD-fed animals revealed a significant decrease in the size of adipocytes in both the epididymal and retroperitoneal WAT of $pRb^{ad-/-}$ animals as compared with the hypertrophied adipocytes observed in the WAT of $pRb^{adL2/L2}$ mice (Fig. 1*H*, *a* and *d*). Interestingly, the WAT of $pRb^{ad-/-}$ contained areas with uni- and multilocular cells, rather characteristic of brown adipocytes (Fig. 1*Hb*). Compared with control animals, $pRb^{ad-/-}$ animals showed an increased number of mitochondria in their WAT, as evidenced by immunohistochemistry using an antibody against Optic Atrophy-1 (OPA-1), a profusion dynamin-related protein of the inner mitochondrial membrane (22), suggesting the presence of BAT-like cells within the WAT of $pRb^{ad-/-}$ animals (Fig. 1*H*, *e* and *f*). BAT of $pRb^{adL2/L2}$ animals on HFD showed lipid accumulation as suggested by vacuolization (Fig. 1*Hg*), an effect which was not observed in the BAT of $pRb^{ad-/-}$ mice (Fig. 1*Hh*). Consistent with the reduced liver weight, Oil red-O (ORO) staining of liver sections

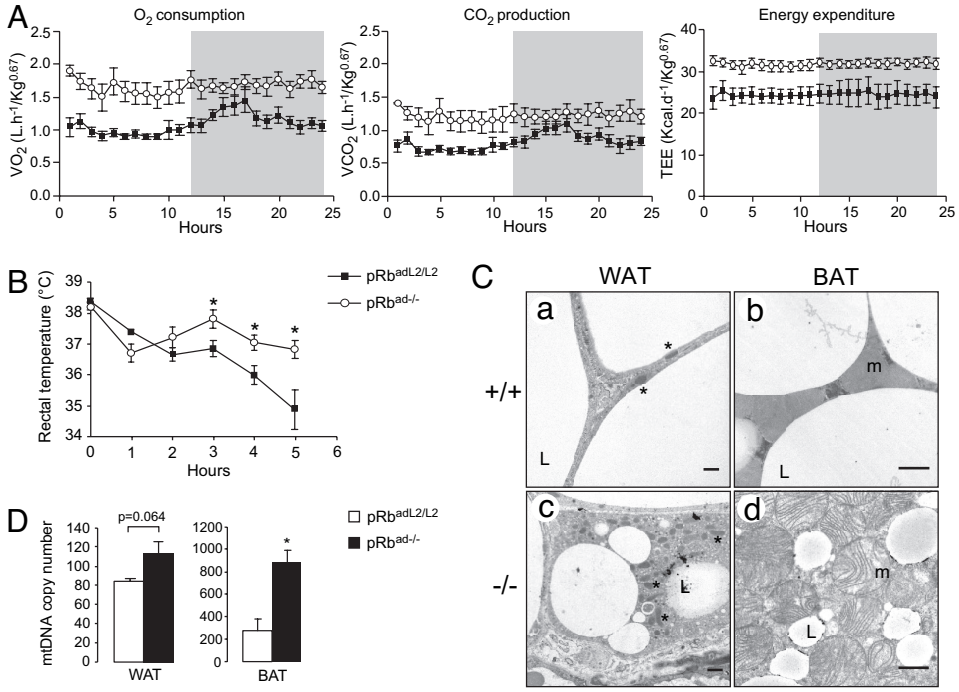

Fig. 2. pRb deficiency increases energy expenditure. (*A*) O_2 consumption, CO_2 production, and total energy expenditure [TEE, calculated from the rate of CO_2 production (VCO_2) and the respiratory quotient (RQ)] in mutant $pRb^{ad-/-}$ ($n = 3$, open circles) and control $pRb^{adL2/L2}$ ($n = 4$, filled squares) mice after 6 weeks on HFD. O_2 consumption and CO_2 production were normalized to (body weight)$^{0.67}$ and measured during 12 h in light cycle and 12 h in the dark phase (shaded area). (*B*) Time course of rectal temperature in $pRb^{ad-/-}$ (open circles) and $pRb^{adL2/L2}$ (filled squares) mice maintained at 4°C. (*C*) Transmission electron micrographs of osmium tetroxide-stained WAT (*a* vs. *c*) and BAT (*b* vs. *d*) ultrathin sections of $pRb^{ad-/-}$ versus $pRb^{adL2/L2}$ mice. (Scale bars: *a* and *c*, 2 μm; *b* and *d*, 1 μm.) * and m, mitochondria; L, lipid droplets. (*D*) mtDNA content in WAT and BAT of $pRb^{adL2/L2}$ and $pRb^{ad-/-}$ mice ($n = 3$).

from $pRb^{adL2/L2}$ animals indicated the presence of many lipid droplets (Fig. 1*Hi*), which was in sharp contrast to the liver of $pRb^{ad-/-}$ mice, where very few and only small lipid droplets were seen (Fig. 1*Hj*).

By using indirect calorimetry, $pRb^{ad-/-}$ mice showed an increase in O_2 consumption and CO_2 production, indicating a higher total energy expenditure (TEE) as compared with control animals (Fig. 2*A*). $pRb^{adL2/L2}$ mice displayed a progressive and significant drop in their body temperature, whereas $pRb^{ad-/-}$ animals maintained their body temperature ≈37°C for up to 5 h in a cold environment (4°C), suggesting an increase in adaptive thermogenesis (Fig. 2*B*). Many of these observations could be explained by mitochondrial activation. We therefore sought to confirm this finding by transmission electron microscopy analysis of WAT and BAT. In the white adipocytes of $pRb^{adL2/L2}$ mice under HFD, few mitochondria were visible and large lipid droplets occupied the cytoplasm (Fig. 2*Ca*). This finding was opposed to the WAT of $pRb^{ad-/-}$ mice, where numerous mitochondria were observed and lipid droplets were significantly smaller (Fig. 2*Cc*). In the HFD-fed $pRb^{ad-/-}$ mice, the brown adipocytes also contained many more mitochondria which had more lamellar crisae and a reduced number of smaller lipid droplets compared with $pRb^{adL2/L2}$ mice (Fig. 2*C*, *b* and *d*). This increase in the number of mitochondria in both WAT and BAT coincides with an increase in mtDNA copy number (Fig. 2*D*).

pRb Deletion in Adipose Tissue Induces Genes Involved in Mitochondrial Activation. To understand the molecular mechanisms underlying the mitochondrial activation in WAT and BAT, we analyzed the expression of genes involved in energy homeostasis and metabolism by using quantitative real-time PCR. In WAT of $pRb^{ad-/-}$ mice, pRb was decreased by 4.5-fold as compared with the $pRb^{adL2/L2}$ controls (Fig. 3). The expression of PGC-1α, a cofactor that controls mitochondrial biogenesis, was significantly induced (23). Furthermore, the expression of the nuclear respiratory factor 1(NRF1) and of the estrogen-related receptor α (ERRα), which mediate some of the effects of PGC-1α on mitochondrial function (24), were induced or had a tendency to be increased in the WAT

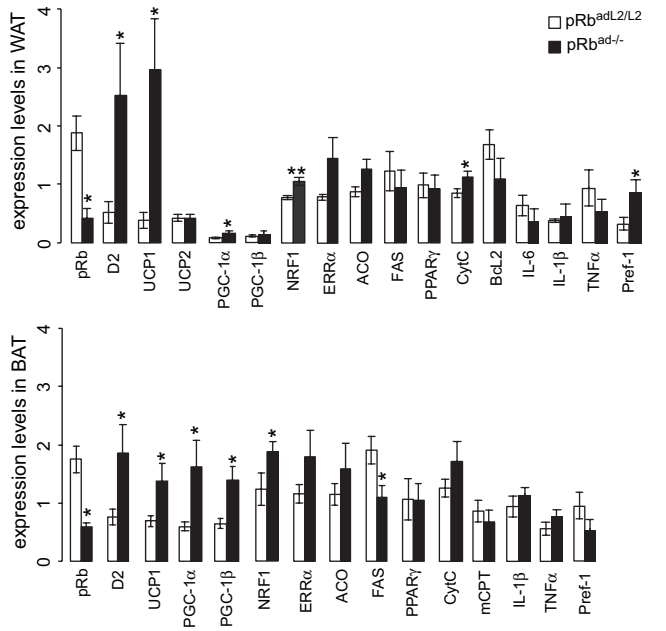

Fig. 3. Genes expression profiles in WAT and BAT of $pRb^{ad-/-}$ mice. Relative mRNA expression levels of the indicated genes in WAT and BAT of $pRb^{ad-/-}$ ($n = 5$) and $pRb^{adL2/L2}$ ($n = 6$) mice after HFD. *, $P < 0.05$; **, $P < 0.01$. D2, type 2 iodothyronine deiodinase.

PHYSIOLOGY

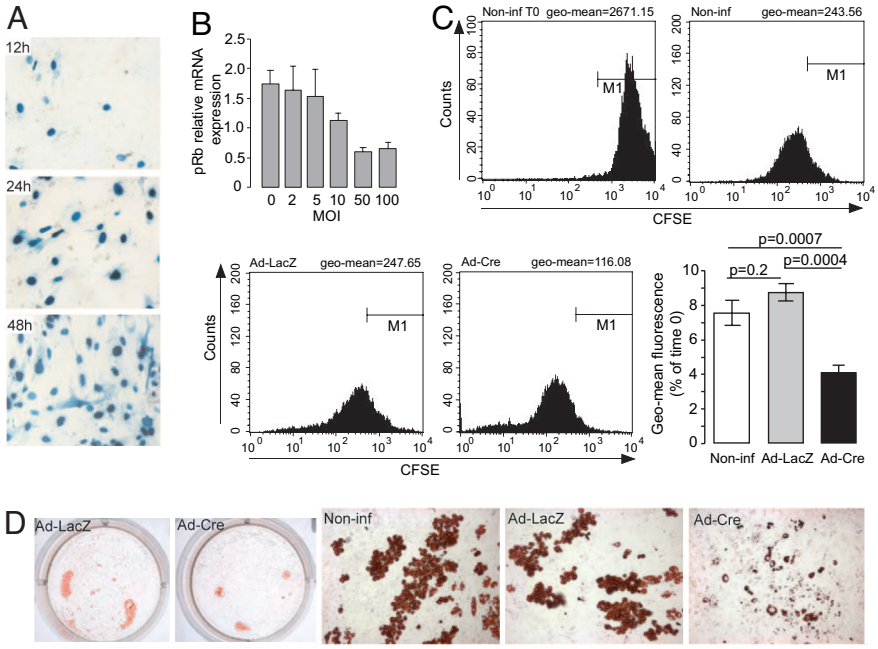

Fig. 4. pRb reduction increases MEFs proliferation and decreases differentiation. (*A*) Ad-LacZ and Ad-Cre coinfected MEFs stained with β-galactosidase after 12, 24, and 48 h of culture. (*B*) Relative mRNA expression of pRb in Ad-Cre-infected $pRb^{L2/L2}$ MEFs at different multiplicities of infection (MOI). (*C*) FACS analysis of noninfected MEFs and MEFs infected with either Ad-LacZ or Ad-Cre and cultured for 48 h in the presence of a fluorescent CFSE dye. The decrease in CFSE mean fluorescence indicates cell division, and geometric mean fluorescence is inversely proportional to the proliferation rate. CFSE staining diagrams are presented from one representative experiment. (*D*) ORO staining of terminally differentiated noninfected $pRb^{L2/L2}$ MEFs and $pRb^{L2/L2}$ MEFs infected with Ad-LacZ or Ad-Cre.

of $pRb^{ad-/-}$ mice. The expression of the PGC-1α transcriptional target UCP1, which is usually not expressed in WAT, as well as the expression of the cytochrome *c* (Cyt *c*), were increased in $pRb^{ad-/-}$ as compared with control WAT. Also, the expression of the type 2 iodothyronine deiodinase (D2), the enzyme that converts T4 into the active thyroid hormone T3 and which plays an important role in adaptive thermogenesis in the BAT (25), was also strongly enhanced in WAT. Systemic T3 hormone levels were, however, not changed in $pRb^{ad-/-}$ as compared with control animals (0.65 ± 0.10 vs. 0.58 ± 0.13 nmol/liter in females and 1.24 ± 0.10 vs. 1.26 ± 0.16 nmol/liter in males). Interestingly, the expression of the preadipocyte marker Pref-1 was enhanced, perhaps pointing toward the presence of more preadipocytes in the WAT of $pRb^{ad-/-}$ mice.

In BAT, excision of the Rb allele reduced the expression of pRb by 2.9-fold, coinciding with a significant increase in PGC-1α, PGC-1β, nuclear respiratory factor 1, type 2 iodothyronine deiodinase, and UCP1 expression. The expression of fatty acid synthase was significantly decreased in BAT of $pRb^{ad-/-}$ mice. Interestingly, pRb deficiency was not accompanied by an inflammatory response in the WAT and BAT because the expression of inflammatory genes such as IL-1β, IL-6, and tumor necrosis factor α (TNFα) were not affected (Fig. 3 and SI Fig. 8).

pRb Deletion in MEFs Results in Increased Proliferation and Apoptosis. We then evaluated some of the cellular mechanisms that could contribute to the tendency of $pRb^{ad-/-}$ adipocytes to take on more brown adipocyte features, using adenoviral overexpression of the Cre recombinase to acutely decrease pRb expression in MEFs of $pRb^{L2/L2}$ animals. To determine the optimal conditions of adenoviral infection, MEFs were first infected with both an adenovirus expressing LacZ (Ad-LacZ) and an adenovirus that expressed the Cre recombinase (Ad-Cre) for 12, 24, and 48 h at a multiplicity of infection of 50. Effective infection of cells with an Ad-Cre resulted in the Cre-mediated deletion of an interposed stuffer DNA flanked by two loxP sites between the promoter and the coding region of the LacZ gene, allowing its expression (26). In view of the results that demonstrated the most efficacious Cre-mediated excision 48 h after coinfection, we chose to use the 48-h time point for proliferation studies (Fig. 4*A*). Subsequently, MEFs from $pRb^{L2/L2}$ mice were infected when they reached 90% confluency with either the control Ad-LacZ or the Ad-Cre virus and labeled with 5- (and 6)-carboxyfluorescein diacetate succinimidyl ester (CFSE) for 48 h before FACS analysis. Noninfected MEFs were used as an additional control. Cells infected at the multiplicity of infection of 50 showed a significant decrease in pRb expression (Fig. 4*B*). The proliferation rate of Ad-Cre-infected MEFs increased significantly when compared with Ad-LacZ-infected and noninfected cells, as reflected by the significant decrease in the Geo-mean fluorescence of Ad-Cre-infected cells (Fig. 4*C*). This increase in the proliferative potential of Ad-Cre-infected MEFs could correlate with the enhanced number of committed preadipocytes that would eventually differentiate into brown adipocytes.

The adipogenic potential of $pRb^{L2/L2}$ MEFs was then assessed by ORO staining of cells 10 days after the induction of adipogenic differentiation. Interestingly, under these conditions, Ad-Cre-infected $pRb^{L2/L2}$ MEFs displayed a significant decrease in the number of fat-containing white adipocyte-like cells in comparison with noninfected and Ad-LacZ-infected $pRb^{L2/L2}$ MEFs (Fig. 4*D*).

Next, the effect of acute pRb deletion was evaluated on the rate of apoptosis both in cultured MEFs and in WAT *in vivo*. By using annexin V-propidium iodide (PI) staining and subsequent FACS analysis, populations of both annexin V^+PI^- (early apoptotic cells) and annexin V^+PI^+ (late apoptotic cells) Ad-Cre-infected $pRb^{L2/L2}$ MEFs were increased 2-fold as compared with noninfected or Ad-LacZ-infected $pRb^{L2/L2}$ MEFs (Fig. 5*A*). We then injected both $pRb^{L2/L2}$ Cre-ER^{T2}-positive and -negative animals with tamoxifen at the dose of 50 mg/kg per day to induce pRb deletion. Forty-eight hours later, we collected WAT and prepared adipocyte cell suspensions, which were scored for apoptosis *in vivo* using annexin V-PI staining and FACS analysis. In WAT cell suspensions of $pRb^{ad-/-}$ mice of both genders, a significant increase in annexin V^+PI^- and annexin V^+PI^+ cell populations as compared with

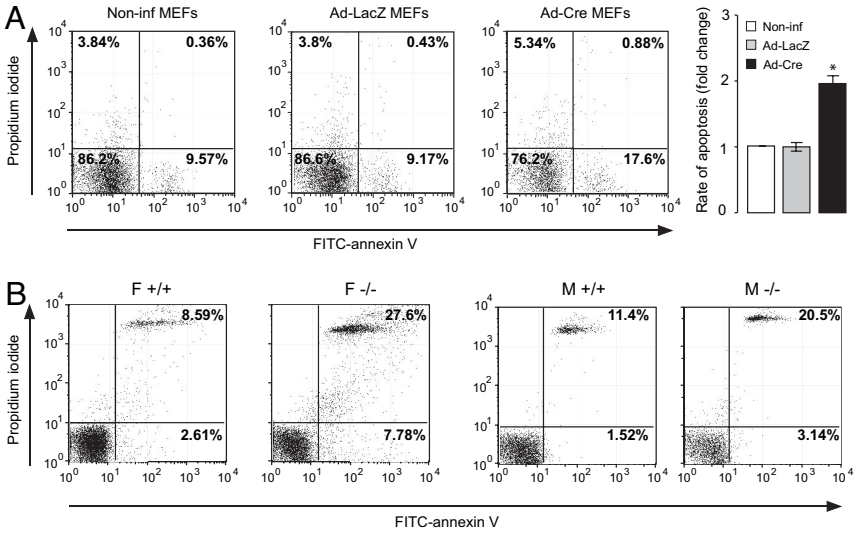

Fig. 5. pRb deficiency increases the apoptosis rate. Flow cytometry analysis of apoptosis in (*A*) noninfected $pRb^{L2/L2}$ MEFs and Ad-LacZ- and Ad-Cre-infected $pRb^{L2/L2}$ MEFs and in (*B*) WAT cell suspension isolated from fat pads of female (F) and male (M) $pRb^{ad-/-}$ and $pRb^{adL2/L2}$ mice 48 h after tamoxifen treatment and staining with annexin V-FITC and PI. The diagrams shown are a representation of three experiments with similar results. *, $P < 0.05$.

$pRb^{adL2/L2}$ controls was observed (Fig. 5*B*), suggesting that *in vivo* apoptosis of mature adipocytes was also enhanced by the absence of pRb.

Discussion

In the present study, we explored the role of pRb in adipocyte biology *in vivo* by using a mouse model in which an adipocyte-specific pRb deficiency was induced in adult mice. Under HFD, the pRb-deficient mice had higher O_2 consumption, produced more CO_2, and displayed an increased thermogenesis as compared with control animals, suggesting an accentuated energy expenditure. Under HFD, as expected, $pRb^{adL2/L2}$ control mice progressively gained weight, whereas $pRb^{ad-/-}$ animals remained lean. In the pRb-deficient animals, areas with BAT features were identified within the WAT, which contrasted with WAT of $pRb^{adL2/L2}$ control mice that displayed hypertrophied white adipocytes. These data are corroborated by the increase in mitochondrial DNA content, by the induction of mitochondrial genes, and by ultrastructural analysis of WAT, which demonstrated the presence of cells containing many mitochondria and small lipid droplets characteristic of brown adipocytes within the WAT of $pRb^{ad-/-}$ mice. The presence of mitochondrial activation within the WAT seen in these $pRb^{ad-/-}$ mice is reminiscent to the phenotype of animals with germ-line deletions of the cofactor RIP140 (27) or the 40S ribosomal protein S6 kinase (28). Also, the BAT of pRb-deficient mice contained less lipids and more mitochondria, suggestive of an enhanced metabolic activity. This enhanced energy expenditure, both in WAT and BAT, underpins the protection against obesity and hepatosteatosis observed in the $pRb^{ad-/-}$ mice. Recently, a very similar phenotype was described in mice lacking another member of the Rb family of pocket proteins, p107. $p107^{-/-}$ animals are leaner than $p107^{+/+}$ littermates with a significant decrease in fat pad mass reminiscent of our data in $pRb^{ad-/-}$ mice (11).

To understand the mechanism underlying the decreased adiposity observed in the pRb-deficient animals, we studied the gene expression pattern in the WAT and BAT in $pRb^{ad-/-}$ and $pRb^{adL2/L2}$ mice. Both in the WAT and BAT of $pRb^{ad-/-}$ animals, a significant increase in the expression of genes known to promote mitochondrial energy expenditure and thermogenesis, such as PGC-1α, nuclear respiratory factor 1, and UCP1, was observed (23). Consistent with our data, it was recently shown in transfection experiments that pRb negatively regulates PGC-1α promoter activity (11). Likewise, MEFs lacking pRb, but not p107/p130 double-deficient MEFs, have an enhanced PGC-1α expression (13). These data hence suggest that pocket proteins, such as pRb, suppress the PGC-1α promoter and are compatible with the induction of PGC-1α expression observed *in vivo* in our study. Furthermore, type 2 iodothyronine deiodinase gene expression was also strongly enhanced in both WAT and BAT of $pRb^{ad-/-}$ animals. As disruption of this gene impairs adaptive thermogenesis (25, 29), the increase in type 2 iodothyronine deiodinase expression hence likely also contributes to the increased thermogenesis observed in $pRb^{ad-/-}$ animals. In combination, these findings support the morphological and physiological phenotype in $pRb^{ad-/-}$ mice, with enhanced mitochondrial activity and increased energy expenditure.

Another mechanism that could contribute perhaps to a lesser extent to the reduced weight gain in $pRb^{ad-/-}$ mice is apoptosis of white adipocytes. As soon as 5 days after the first tamoxifen injection, the body fat content of $pRb^{ad-/-}$ animals was modestly, yet significantly, decreased as compared with $pRb^{adL2/L2}$ animals (Fig. 1*B*). This early decrease in fat mass could be, at least in part, due to the increased rate of apoptosis of white adipocytes as demonstrated by an enhanced apoptosis in WAT cell suspensions after the induction of pRb deletion. The early decrease in body fat content is probably not due to a differentiation defect of adipose tissue precursors, because such cells require a longer period to achieve full terminal differentiation. In agreement with previous studies in which low levels of pRb coincide with an enhanced rate of apoptosis (30–33), a similar increase in the rate of apoptosis was also found in pRb-deficient MEFs as compared with control MEFs.

pRb is well known to arrest cell proliferation by interacting with E2F transcription factors and blocking the progression of the cell cycle (34). In this report we have shown that MEFs in which the pRb gene was partially deleted by Ad-Cre infection proliferate faster in comparison with noninfected or Ad-LacZ-infected MEFs. Although it is not presumptuous to speculate that the formation of the BAT-like tissue within the WAT results from a partial transdifferentiation of existing white adipocytes, an increase in the proliferation of committed preadipocytes, as evidenced by the increase in the expression of the preadipocyte marker Pref-1 in the WAT, which could later preferentially differentiate into brown adipocytes, could also contribute to the phenotype. Consistent with this last hypothesis, we (Fig. 4*D*) and others (11, 13) have shown that $pRb^{-/-}$ MEFs did not differentiate appropriately into adipocytes

PHYSIOLOGY

that accumulate fat when stimulated with adipocyte differentiation mix, as is the case for the control MEFs. These data are also in line with earlier immunohistochemical experiments, which show that pRb immunoreactivity was absent from brown adipocyte precursors, whereas pRb was expressed in lipid droplet-containing white adipocyte precursors (13).

In conclusion, this study demonstrates *in vivo* the essential and direct role of pRb in adipocyte cell fate determination. The absence of pRb in adipocytes enhanced mitochondrial activity in both WAT and BAT. Furthermore, WAT takes on many more BAT-like features, which positions it well to contribute to energy expenditure and the maintenance of energy homeostasis. In view of these data, the retinoblastoma protein is well placed to eventually become a therapeutic target aimed at inducing weight loss in obese patients.

Materials and Methods

Animals Experiments. $pRb^{L2/+}$ (20) and aP_2-$CreER^{T2}$ (21) on a C57BL6/J background (six backcrosses) were intercrossed to generate cohorts of $n = 8$ mice per group that have the following genotypes: $pRb^{L2/L2} \times aP_2$-$CreER^{T2(Tg/0)}$ and $pRb^{L2/L2} \times aP_2$-$CreER^{T2(0/0)}$. Mice in which pRb was inactivated after tamoxifen injection will be referred to as $pRb^{ad-/-}$, and their controls will be referred to as $pRb^{adL2/L2}$. All mice were maintained in a temperature-controlled (23°C) facility with a 12-h light/dark cycle and were given free access to food and water. The control diet (EQ12310) and the HFD (EQ/D12309) were from UAR (Villemoison sur Orge, France). The mice were fasted 4 h before harvesting blood and tissue collection. Body fat mass was evaluated in anesthetized mice by dual energy x-ray absorptiometry (PIXIMUS; GE Medical Systems, Buc, France). Indirect calorimetry was performed exactly as described (35).

Histology, Immunohistochemistry, and Electron Microscopy. WAT, BAT, and liver tissues were prepared and stained with H&E and ORO as described (29). Immunohistochemistry was used to detect Optic Atrophy-1 (OPA-1) (22) with an OPA-1 antibody (dilution 1:1,000) that was kindly provided by C. Alexander (Max Delbrück Center for Molecular Medicine, Berlin, Germany). Electron microscopy was performed as described (36).

Gene Expression and Mitochondrial DNA Content Analyses. Expression levels were analyzed on cDNA synthesized from total mRNA by using quantitative real-time PCR, and mitochondrial DNA content was quantified in WAT and BAT as described (35). The sequences of the primer sets used are available in SI Table 1.

Cell Culture, Proliferation, and Apoptosis Assays. MEFs were prepared from $pRb^{adL2/L2}$ embryos at embryonic day 13.5 and self-immortalized as described (36). $pRb^{L2/L2}$ MEFs were infected for 48 h with either Ad-LacZ or Ad-Cre (RIKEN BioResource Center, Tsukuba, Japan) to induce the deletion of the Rb locus. For proliferation studies, cells were after-deletion labeled with 20 μg/ml of CFSE (Sigma–Aldrich, St. Louis, MO) at 37°C for 15 min and washed. Cells were then split, and one plate was immediately fixed in 2% paraformaldehyde for 15 min at 4°C and prepared for time 0 (T_0) fluorescence determination. The other half of the cells were cultured at a density of 10^6 cells for 48 h in DMEM containing 10% newborn calf serum to allow cell proliferation. After 48 h, cells were collected, washed in PBS, and then analyzed by FACS.

For determination of apoptosis, MEFs were collected 48 h after gene deletion, washed in PBS-2% BSA, and stained with FITC-conjugated annexin V and PI in RPMI medium 1640 for 5 min at 21°C. Data for proliferation or apoptosis were collected with a FACSCalibur (Becton Dickinson Biosciences, San Jose, CA) and analyzed by the FlowJo software (Tree Star, Ashland, OR). Cell culture experiments were repeated three times. Representative experiments were shown.

For *in vivo* apoptosis assay, 6- to 8-week-old $pRb^{L2/L2}/aP_2$-$CreER^{T2(Tg/0)}$ mice and their controls were injected with tamoxifen. After 48 h, WAT was removed and single-cell suspensions were prepared. WAT cells were gently dissociated in PBS-2% BSA, centrifuged, and transferred into RPMI medium 1640 containing ammonium chloride to lyse red blood cells. Cells were then washed in RPMI medium 1640, incubated with FITC-conjugated annexin V and PI (BD PharMingen, San Jose, CA) in RPMI medium 1640 for 5 min at 21°C, and then analyzed by FACS.

We acknowledge Dr. Anton Berns for the generous gift of mice with a floxed Rb allele. We are grateful to M. Selloum, C. Alexander, and members of the J.A. laboratory for technical assistance, gift of materials, and helpful discussions. This work was supported by grants from the Centre National de la Recherche Scientifique, Institut National de la Santé et de la Recherche Médicale, National Institutes of Health, European Union, and the Hôpitaux Universitaires de Strasbourg.

1. Nguyen DX, McCance DJ (2005) *J Cell Biochem* 94:870–879.
2. Lipinski MM, Jacks T (1999) *Oncogene* 18:7873–7882.
3. Chau BN, Wang JY (2003) *Nat Rev Cancer* 3:130–138.
4. Vooijs M, Berns A (1999) *Oncogene* 18:5293–5303.
5. Jacks T, Fazeli A, Schmitt EM, Bronson RT, Goodell MA, Weinberg RA (1992) *Nature* 359:295–300.
6. Lee EY, Chang CY, Hu N, Wang YC, Lai CC, Herrup K, Lee WH, Bradley A (1992) *Nature* 359:288–294.
7. Clarke AR, Maandag ER, van Roon M, van der Lugt NM, van der Valk M, Hooper ML, Berns A, te Riele H (1992) *Nature* 359:328–330.
8. Thomas DM, Carty SA, Piscopo DM, Lee JS, Wang WF, Forrester WC, Hinds PW (2001) *Mol Cell* 8:303–316.
9. Balsitis SJ, Sage J, Duensing S, Munger K, Jacks T, Lambert PF (2003) *Mol Cell Biol* 23:9094–9103.
10. Ruiz S, Santos M, Segrelles C, Leis H, Jorcano JL, Berns A, Paramio JM, Vooijs M (2004) *Development (Cambridge, UK)* 131:2737–2748.
11. Scime A, Grenier G, Huh MS, Gillespie MA, Bevilacqua L, Harper ME, Rudnicki MA (2005) *Cell Metab* 2:283–295.
12. Chen PL, Riley DJ, Chen Y, Lee WH (1996) *Genes Dev* 10:2794–2804.
13. Hansen JB, Jorgensen C, Petersen RK, Hallenborg P, De Matteis R, Boye HA, Petrovic N, Enerback S, Nedergaard J, Cinti S, *et al.* (2004) *Proc Natl Acad Sci USA* 101:4112–4117.
14. Classon M, Kennedy BK, Mulloy R, Harlow E (2000) *Proc Natl Acad Sci USA* 97:10826–10831.
15. Higgins C, Chatterjee S, Cherington V (1996) *J Virol* 70:745–752.
16. Fajas L, Egler V, Reiter R, Hansen J, Kristiansen K, Debril MB, Miard S, Auwerx J (2002) *Dev Cell* 3:903–910.
17. Nikitin A, Shan B, Flesken-Nikitin A, Chang KH, Lee WH (2001) *Cancer Res* 61:3110–3118.
18. Richon VM, Lyle RE, McGehee RE, Jr. (1997) *J Biol Chem* 272:10117–10124.
19. Ross SR, Choy L, Graves RA, Fox N, Solevjeva V, Klaus S, Ricquier D, Spiegelman BM (1992) *Proc Natl Acad Sci USA* 89:7561–7565.
20. Marino S, Vooijs M, van Der Gulden H, Jonkers J, Berns A (2000) *Genes Dev* 14:994–1004.
21. Imai T, Jiang M, Chambon P, Metzger D (2001) *Proc Natl Acad Sci USA* 98:224–228.
22. Frezza C, Cipolat S, Martins de Brito O, Micaroni M, Beznoussenko GV, Rudka T, Bartoli D, Polishuck RS, Danial NN, De Strooper B, Scorrano L (2006) *Cell* 126:177–189.
23. Puigserver P, Spiegelman BM (2003) *Endocr Rev* 24:78–90.
24. Mootha VK, Handschin C, Arlow D, Xie X, St Pierre J, Sihag S, Yang W, Altshuler D, Puigserver P, Patterson N, *et al.* (2004) *Proc Natl Acad Sci USA* 101:6570–6575.
25. de Jesus LA, Carvalho SD, Ribeiro MO, Schneider M, Kim SW, Harney JW, Larsen PR, Bianco AC (2001) *J Clin Invest* 108:1379–1385.
26. Kanegae Y, Lee G, Sato Y, Tanaka M, Nakai M, Sakaki T, Sugano S, Saito I (1995) *Nucleic Acids Res* 23:3816–3821.
27. Leonardsson G, Steel JH, Christian M, Pocock V, Milligan S, Bell J, So PW, Medina-Gomez G, Vidal-Puig A, White R, Parker MG (2004) *Proc Natl Acad Sci USA* 101:8437–8442.
28. Um SH, Frigerio F, Watanabe M, Picard F, Joaquin M, Sticker M, Fumagalli S, Allegrini PR, Kozma SC, Auwerx J, Thomas G (2004) *Nature* 431:200–205.
29. Watanabe M, Houten SM, Mataki C, Christoffolete MA, Kim BW, Sato H, Messaddeq N, Harney JW, Ezaki O, Kodama T, *et al.* (2006) *Nature* 439:484–489.
30. Fajas L, Egler V, Reiter R, Miard S, Lefebvre AM, Auwerx J (2003) *Oncogene* 22:4186–4193.
31. Lefebvre M, Paulweber B, Fajas L, Woods J, McCrary C, Colombel JF, Najib J, Fruchart JC, Datz C, Vidal H, *et al.* (1999) *J Endocrinol* 162:331–340.
32. Yamamoto H, Soh JW, Monden T, Klein MG, Zhang LM, Shirin H, Arber N, Tomita N, Schieren I, Stein CA, Weinstein IB (1999) *Clin Cancer Res* 5:1805–1815.
33. Guy M, Moorghen M, Bond JA, Collard TJ, Paraskeva C, Williams AC (2001) *Br J Cancer* 84:520–528.
34. Helin K (1998) *Curr Opin Genet Dev* 8:28–35.
35. Lagouge M, Argmann C, Gerhart-Hines Z, Meziane H, Lerin C, Daussin F, Messadeq N, Milne J, Lambert P, Elliott P, *et al.* (2006) *Cell* 127:1109–1122.
36. Picard F, Gehin M, Annicotte J, Rocchi S, Champy MF, O'Malley BW, Chambon P, Auwerx J (2002) *Cell* 111:931–941.